Modeling black spruce wood fiber attributes with terrestrial laser scanning

Guillaume Giroud [a] *
Robert Schneider [b]
Richard A. Fournier [c]
Joan E. Luther [d]
Olivier Martin-Ducup [e]

[a] Direction de la recherche forestière, Ministère des Forêts, de la Faune et des Parcs du Québec, 2700 Einstein, Québec, QC G1P 3W8, Canada.
[b] Chaire de recherche sur la forêt habitée, Département de biologie, chimie et géographie, Université du Québec à Rimouski (UQAR), 300 allée des Ursulines, Rimouski, Québec G5L 3A1, Canada.
[c] Department of Applied Geomatics, Centre d'applications et de recherches en télédétection (CARTEL), Université de Sherbrooke, 2500, boul. de l'université, Sherbrooke, Québec J1K 2R1, Canada.
[d] Natural Resources Canada, Canadian Forest Service – Atlantic Forestry Centre, 26 University Drive, Corner Brook, NL A2H 5G5, Canada.
[e] Institut de recherche pour le développement (IRD), UMR AMAP, Montpellier, France.
* Corresponding author.

E-mail addresses: Guillaume.Giroud@mffp.gouv.qc.ca, Robert.Schneider@uqar.ca, Richard.Fournier@USherbrooke.ca, joane.luther@canada.ca, olivier.martin@ird.fr

Abstract

A model comparison approach, based on the Akaike's information criterion, was used to evaluate the contribution of terrestrial laser scanning (TLS) to the estimation of wood fiber attributes at the tree level for black spruce (*Picea mariana* (Mill.) B.S.P.) trees growing in Newfoundland, Canada. Substantial efforts were made to acquire, process, and develop accurate and detailed metrics of the tree, its crown, and its immediate environment. Based on the resulting data set, significant relationships were found, and models were successfully developed, using only TLS metrics, for predicting wood fiber attributes. The models accounted for 47%, 33%, 51%, 44%, and 52% of variance in wood density, coarseness, fiber length, microfibril angle, and modulus of elasticity respectively, with root mean square error values of 46 kg/m^3, 37 µg/m, 0.20 mm, 3.5 º, 2.3 GPa. Our ability to estimate the wood fiber attributes was improved by combining TLS metrics with conventional field measurements. This study demonstrates that the use of TLS metrics improves the estimation of the wood fiber attributes at the tree level beyond that possible with conventional field measurements.

Keywords: forest inventory, terrestrial laser scanning, modeling of wood fiber attributes, non-destructive measurement of trees, black spruce boreal forest.

Introduction

Newfoundland and Labrador's forest products industry directly and indirectly employs over 5,500 workers in pulp and paper, sawmilling, harvesting, and value-added sectors (Government of Newfoundland and Labrador 2015; 2018a). The pulp and paper sector accounts for approximatively 50% of total revenues and uses 1.2 million cubic meters of local timber, predominantly balsam fir (*Abies balsamea* (L.) Mill.) and black spruce (*Picea mariana* (Mill.) B.S.P.). The fiber attributes of both species greatly influence the processing, quality, and uniformity of the end products. For example, refining black spruce pulp requires more energy because of its higher density and longer fibers (Li et al. 2011). Black spruce also produces thermomechanical pulping with significantly higher strength properties, whereas balsam fir provides superior optical properties because of its lower cell wall thickness. However, the supply is never consistent in quality because the fiber attributes vary locally and spatially for a given species, as shown for black spruce in eastern Canada (Lessard et al. 2014; Giroud et al. 2017). Defo et al. (2015) recently noted the importance of knowing the quantity and quality of the forest resource for matching the right fiber to the right end use to maximize product value and also to understand the effects of our forest management decisions on wood quality.

Wood fiber quality is determined by intrinsic wood properties. One growth ring is produced each year, consisting of a zone of earlywood followed by a zone of latewood (Larson 1969). Latewood is characterized by denser cells with a lower microfibril angle (MFA) (Donaldson 2008). The local growth conditions either directly or indirectly influence the crown development, and consequently, the width of the growth rings and the relative proportion of earlywood to latewood within the rings. The link between tree characteristics and wood fiber attributes is often limited, but significant, at the tree level. In 1984, Alemdag reported weak relationships between wood density and diameter at breast height (DBH), total height, and age for black spruce and 27 other species in Ontario, Canada. More recently, Giroud et al. (2017) observed weak correlations between wood density, modulus of elasticity (MOE), and stem characteristics for the main boreal species of Quebec, including black spruce. Similar correlations were found between wood density and crown characteristics for black spruce and balsam fir in Newfoundland (Groot and Luther 2015). Groot et al. (2015) suggested that the weakness of the relationship between crown characteristics and wood density could be a consequence of the relatively simple description of the tree crown (width, length, and ratio) in conventional inventories. Groot et al. (2015) also suggested this limitation could be addressed with remote sensing technologies that measure the crowns more accurately. Airborne and terrestrial laser scanning (ALS and TLS) can provide a wide range of forest metrics for modeling purposes. The proof-of-concept was recently demonstrated for balsam fir and black spruce with the prediction of plot-level wood fiber attributes using only ALS data as covariates (Luther et al. 2014; Pokharel et al. 2016). Wood fiber attribute models were also successfully developed for balsam fir and black spruce in Newfoundland using a suite of local structural metrics derived from TLS data (Blanchette et al. 2015). Terrestrial laser scanning can also provide metrics such as crown competition indices at the tree level (Martin-Ducup et al. 2016).

In this study, wood fiber attribute estimation was further investigated at the tree level for black spruce trees growing in Newfoundland, Canada. More specifically, objectives were to (i) establish a set of metrics to characterize the tree, its crown, and its immediate environment using TLS data; (ii) develop a list of candidate models, with and without TLS metrics, to estimate the basic density, coarseness, fiber length, MOE, and MFA; (iii) and compare these models and determine the contribution of TLS for modeling wood fiber attributes. The study focused on key fiber attributes that were identified, following a broad consultation of experts across Canada, as key important attributes for industry (Natural Resources Canada 2010). Although Blanchette et al. (2015) demonstrated the potential of TLS for modeling wood fiber attributes at the plot level, to our knowledge, this is the first study to model these attributes at the tree level using metrics derived from TLS data.

Materials and methods

Study area and data collection

The island of Newfoundland is the easternmost region of Canada. The boreal forest cover makes up about 46% of its total area (111,390 km^2), the remainder consisting of lakes, rivers, and wetlands (Government of Newfoundland and Labrador 2018b). Newfoundland's forests are mainly dominated by balsam fir and black spruce, mixed with some hardwoods. Black spruce accounts for approximately one-third of the forests of the island. This slow-growing species grows in a variety of conditions, including very wet and dry soils. Black spruce is the dominant species across much of central Newfoundland, where forest fires are more common. Elsewhere, forests are dominated by balsam fir in pure or mixed stands.

Data used were a subset of a larger data set collected and analyzed as part of the Newfoundland Fibre Inventory Project (Lessard et al. 2014; Luther et al. 2014). In the current study, 16 sites representing black spruce growing in mature stands of medium site quality were retained. Table 1 shows site location and characteristics. A total of ten merchantable-sized black spruce trees per site were initially core sampled to measure the wood fiber attributes. Field data were collected on these trees, including diameter at breast height (DBH), total tree height, and crown measurements as described by Groot and Luther (2015; Table 2). Crown length was determined by subtracting base of live crown from total tree height. Crown radius was computed as the average value of two crown width measurements (North–South and East–West). Crown surface area was determined from crown radius and crown length, assuming a conical crown. Crown density was assessed on a scale of 1 to 3, with 1 representing >66% density and 3 <33% density. Basal area of larger trees (BAL) was calculated by comparing DBH of cored trees with the DBH distribution.

Terrestrial laser scanning data acquisition and processing is described in Blanchette et al. (2015). The TLS scans were acquired using a Z+ F Imager® 5006i (Zoller + Fröhlich GmbH, Wangen im Allgäu, Germany) operated at 0.036° angular resolution. Each site was scanned using four peripheral and one central viewpoints in order to include as many cored trees as possible, reducing signal occlusion (Fig. 1). Each scan was aligned with circular black and white targets. Six targets were visible from the central viewpoint, whereas a minimum of three visible targets was required for each peripheral scan location. A filtering procedure was also applied to remove all noise points using Z+F LaserControl® version 8.1.3 (Zoller + Fröhlich GmbH). The TLS scene including all the cored trees was about 25 m × 25 m using this protocol. Because of the occlusion and scanning limitations in forests, not all the cored trees were visible within a TLS scene. The final data set consisted of 69 visible cored trees (hereafter referenced as “target” trees) from 16 different sites.

Tree-level metrics derived from TLS point clouds

Conventional inventories do not measure competition and terrain features at the tree level, and description of the crown, when made, is highly simplified (Groot et al. 2015). Tree-level metrics were derived from TLS point clouds to describe as precisely as possible the tree, its crown, and its immediate environment in terms of competition and local topography (Table 2). Cylinders were thus isolated from the TLS scenes using a semi-automatic procedure in the Computree platform version 3.0 (Othmani et al. 2011; Fig. 2). The cylinder diameter (*Ø*) was estimated as a function of the highest point of the canopy (*Canopy_MAX*) inside an upside-down cone placed at the tree base with a 30° opening angle. This angle value was chosen by trial and error to obtain a representative area for the computed metrics according to the canopy height. Highest point of the canopy and coordinates (x, y, z) of each tree base were manually measured using FARO® SCENE version 5.0.1 (Faro Technologies Inc., Lake Mary, Florida, USA).

$$\text{Ø}_i = 2\tan(15°)\text{Canopy\_MAX}_i \quad (1)$$

where $Ø_i$ is the estimated diameter of cylinder *i*, and $Canopy\_MAX_i$ is the highest point of the canopy of cylinder *i*.

A suite of metrics was computed to describe the canopy structure and the local topography within the cylinders as detailed by Blanchette et al. (2015). A Digital elevation model (DEM), digital surface model (DSM), and canopy height model (CHM) were computed for each cylinder scene using a grid of 25 cm x 25 cm resolution with TIFFS© version 8.0 beta (Globalidar, Honolulu, Hawaii, USA). This resolution was chosen to reduce the amount of data while retaining as much detail as possible. Mean and standard deviations of the canopy model (CHM_MEAN, CHM_STD) were extracted to describe the canopy height and its level of variance. Canopy surface roughness was estimated by a rumple index (CHM_RUMPLE) computed as the ratio of the 3D canopy surface over its 2D projection (Kane et al. 2010). Vegetation density was estimated by a volume-to-area ratio index (CHM_RATIO) computed as the volume present between the reference plane given by the DEM and the DSM surface. Relative elevation difference was calculated as the difference between the lowest and highest points of the DEM within the cylinder (DEM_EL_DIF). Standard deviation of elevation (DEM_EL_STD) was also determined. A rumple index was computed in the same manner as for the canopy to characterize the ground surface roughness (DEM_EL_RUMPLE). The mean slope and its standard deviation were also estimated within each cylinder from the DEM (DEM_SL_MEAN, DEM_SL_STD).

A suite of metrics was then computed to characterize the stem competition within the cylinders as detailed by Blanchette et al. (2015). One-meter thick slices centered at 1.5 m above ground were extracted from each scene (Huang et al. 2009). Each slice was manually filtered to keep only the points from circular sections related to the trunks of standing trees. The location of each standing tree was manually recorded using PointStream© version 3.0, as a point cloud viewer (Arius Technology Inc., Vancouver, British Columbia, Canada). Stem density (TLS_STEMS) was computed within the cylinders. Using the stem coordinates, the observed average distance between neighbors (TLS_DISTANCE) was also calculated (Blanchette et al. 2015). An aggregation index was then computed as the ratio of the observed versus expected distance between neighbors (TLS_RATIO) (Clark and Evans 1954). This metric provides a direct measure of “dispersion” or “clustering” of stems surrounding each target tree. The smaller the ratio, the higher the competition for space among neighboring trees.

The target trees were then isolated from the cylinders using a semi-automatic procedure in Computree platform version 3.0 (Othmani et al. 2011; Fig. 2). Tree height (TLS_TH), base of live crown (TLS_CR_BLC), and crown length (TLS_CR_LGT) were manually measured using FARO® SCENE version 5.0.1 (Faro Technologies Inc.). The points belonging to the crown of each target tree were exported from Computree. The point clouds were then voxelized using "VoxR" library (Lecigne et al. 2015) and R statistical and programming language version 3.0.2 (R Development Core Team 2018). A voxel size of 10 cm was chosen to represent the geometry of the crown in sufficient detail. A 3D alpha-shape reconstruction was applied to measure the surface (TLS_CR_SA) and volume (TLS_CR_VOL) of each crown using the ''alphashape3d" package in R (Lafarge and Pateiro-Lopez 2017). Crown density (TLS_CR_DEN) was also estimated by dividing the volume of non-empty voxels by the crown volume.

Three indices were computed to characterize the canopy competition within the cylinders as detailed by Martin-Ducup et al. (2016): the canopy pressure index (CPI), the canopy heterogeneity index (CHI), and the canopy density index (CDI). The immediate vegetation surrounding each target tree was isolated from the cylinders using an upside-down cone placed at the crown base with a 30° opening angle (Fig. 2). The point clouds were voxelized using the same 10 cm voxel size as that used on the crowns of the target trees ("VoxR" library, Lecigne et al. 2015). Canopy pressure index was computed as follows:

$$CPI = \frac{1}{n}\sum_{i=1}^{n}\frac{H_i V_i}{d_i} \qquad (2)$$

where n is the number of cells in the raster, V_i is the number of non-empty cells in the Z direction above the raster cell i, d_i is the distance between the cell i and the projected center of the crown, and H_i is the mean height of the voxels of the cell i.

The spatial dispersion of the surrounding vegetation was estimated by the CHI computed as a Clark and Evans aggregation index based on the XY coordinates of each cell of the raster (Clark and Evans 1954). A CDI was also calculated as the ratio between the volume occupied by non-empty voxels and the total volume of the cone.

Analysis of wood fiber attributes

The 12 mm diameter increment cores were extracted at breast height from target trees. Cores were sent to the FPInnovations laboratory in Vancouver, British Columbia. After an acetone extraction, the samples were cut into radial strips of 2 by 7 mm (tangentially by longitudinally), and conditioned at 40% relative humidity and 20°C to reach a wood moisture content of 8%. Pith-to-bark profiles of wood density, stiffness (MOE), MFA, and coarseness were measured using SilviScan^{TM} technology (Evans 1994, 2006). Wood density was determined at 25-µm radial resolution using the X-ray densitometer unit of SilviScan^{TM}. The wood density at 8% moisture content was then converted to basic density (BD), which is the most commonly used definition. Basic density is defined as the ratio between the oven-dry mass of a wood sample and its green volume and was calculated as follows (Siau 1995):

$$\mathrm{BD} = \frac{1000 \times D_8}{1080 + 0.22 \times D_8} \tag{3}$$

where BD is basic density and D_8 is density at 8% moisture content. It is assumed that the fiber saturation point is 30% and that the water density is 1000 kg/m³.

Core measurements, such as the average ring width (RW) and the number of rings (RN), were determined from the density profiles. Microfibril angle was determined by the X-ray diffractometer unit of SilviScan™. Modulus of elasticity was estimated using the density and the coefficient of variation of the X-ray diffraction profile intensity. Coarseness (COA) was calculated by combining the profiles of wood density and tracheid diameter obtained by image analysis with SilviScan™. Fiber length (FL) was also measured at the FPInnovations lab by analyzing a fiber solution made from macerated wood cores with a high-resolution fiber quality analyzer (HiRes FQA, OpTest Equipment Inc., Hawkesbury, Ontario, Canada). The HiRes FQA system collects and analyzes images of fibers from the pulp solution. Length-weighted fiber length was used as it corrects the natural bias associated with fiber-wall fragments, also called fines (Robertson et al. 1999). Depending on the total age of the samples, fiber length was acquired in two or three age classes, corresponding to juvenile wood (age 1–30), transition wood (age 31–60), and mature wood (age 61+). Samples were run in duplicate for each age class, and the results averaged to get a single value by age class. Wood fiber attributes were averaged assuming a circular shape of the rings. Wood fiber attributes are thus average estimates of the stem cross-section at breast height.

Statistical analysis

Pearson's correlations were estimated to assess the strength of linear relationships between the wood fiber attributes (BD, COA, FL, MOE, MFA) and the metrics of the target tree and its immediate environment, measured during the forest inventory or derived from TLS (PROC CORR, SAS 9.3, SAS Institute Inc., Cary, North Carolina, USA). A model comparison approach was then used to ensure that all the potential categories of covariates would be tested for their ability to predict wood fiber attributes. Seven sets of candidate models were retained to evaluate the contribution of different covariate groups: (1) the "CORE" set included the number of rings, the log transformation of the ring number, and the average ring width; (2) the "STEM" set included DBH, tree height, slenderness, and basal area of larger trees; (3) the "STEM+CROWN" set contained all covariates of the "STEM" set plus the crown measurements measured in the field; (4) the "STEM+CROWN+CORE" set contained all covariates of the three sets; (5) the "TLS" set contained all metrics derived from the TLS data; (6) the "STEM+CROWN+TLS" set contained all covariates of the three sets; and (7) the "STEM+CROWN+CORE+TLS" set contained all of the available covariates (Table 2). Within each set of models, all possible combinations were tested up to a maximum of three covariates. Candidate models with strongly correlated covariates were removed. Correlation coefficient >0.8 or <-0.8 was considered as evidence of collinearity between two covariates.

Linear mixed-effects models were developed for estimating the wood fiber attributes at the tree level (PROC MIXED, SAS 9.3, SAS Institute Inc.). A site random effect was added to all models to account for within-site correlation as follows:

$$Y_{ij} = a_0 + a_1 COV1_{ij} + a_2 COV2_{ij} + a_3 COV3_{ij} + u_i + \varepsilon_{ij} \quad (4)$$

Where Y_{ij} is one of the wood fiber attributes of target tree j in site i, a_0 to a_6 the fixed effect parameters, $COV1$ to $COV3$ the three covariates, u_i the normally distributed site random effect parameter ($u_i \sim N(0,\sigma_i^2)$), and ε_{ij} the residual error ($\varepsilon_{ij} \sim N(0,\sigma^2)$).

The models were fitted by maximum likehood to find the best model for the fixed effects. The model with the lowest Akaike's information criterion for small sample size (AICc) was considered as the best model for a given set of covariates (Burnham and Anderson 2003). Delta AICc (ΔAICc) and Akaike weights (ωi) were also computed for model comparison. The parameters of the most parsimonious models were subsequently re-estimated using a restricted maximum likelihood (REML) approach. The goodness of fit was assessed by computing the marginal pseudo-R2 as described by Nakagawa and Schielzeth (2013). The marginal pseudo-R2 is only concerned with variance explained by fixed effects. No model averaging or cross-validation procedures were applied because the objective was only to evaluate the contribution of different sets of covariates for modeling wood fiber attributes at the tree level.

Results

Correlative relationships

Table 3 shows Pearson's correlation coefficients between the wood fiber attributes and the most influential covariates according to our modeling results. A magnitude of between 0.5 and 0.8 usually indicates moderate correlation, whereas a magnitude of more than 0.8 indicates strong correlation. Highly significant correlations were found between the wood fiber attributes and the core measurements. Moderate linear relationships were obtained with the ring number and the log transformation of the ring number (RNLN), with correlation coefficients between 0.47 and 0.63, in absolute values. The fiber attributes increase with age and then stabilize at maturity, except for MFA, which decreases with age until maturity. Moderate linear relationships were also observed with the average ring width, with correlation coefficients between 0.56 and 0.70, in absolute values. The narrower the ring, the lower the MFA and the higher the other fiber attributes.

Many highly significant correlations were found between the wood fiber attributes and the tree measurements (Table 3). Weak to moderate linear relationships were obtained with correlation coefficients between 0.26 and 0.58, in absolute values. Diameter at breast height was negatively related to BD. Tree height (TH) was positively related to fiber length and negatively to MFA. The higher the slenderness ratio (HD), the lower the MFA and the higher the other fiber attributes, except for fiber length (non-significant). Basal area of larger trees (BAL) was positively related to wood density. Base of live crown (CR_BLC) was significantly correlated with all wood fiber attributes. The higher the base of live crown, the lower the MFA and the higher the other fiber attributes. Crown length (CR_LGT) was negatively related to wood density.

Many highly significant correlations were also found between wood fiber attributes and TLS metrics (Table 3). Weak to moderate linear relationships were obtained, with correlation coefficients between 0.24 and 0.65, in absolute values. The wood fiber attributes were more weakly correlated with the base of live crown derived from TLS (TLS_CR_BLC) than with the base of live crown measured in the field (CR_BLC). Crown density (TLS_CR_DEN) was negatively correlated to fiber length. Crown volume (TLS_CR_VOL) was negatively related to wood density. The canopy competition indices derived from TLS (CPI, CHI, CDI) were all positively correlated with wood density. Significant correlations were also found with the heterogeneity and variability of the canopy height model (CHM_RUMPLE, CHM_STD). The more irregular the vertical forest structure, the lower the MFA, and the higher the other wood fiber attributes. Wood fiber attributes were significantly correlated with local topography (DEM_EL_RUMPLE, DEM_SL_MEAN). The more irregular the topography surrounding the target tree, the higher the MFA, and the lower the other fiber attributes. Highly significant correlations were also found with stem competition indices derived from TLS (TLS_RATIO, TLS_DISTANCE). The lower the competition for space among neighboring trees, the higher the MFA, and the lower the other fiber attributes. Similarly, the longer mean distance between trees, the higher the MFA, and the lower the other fiber attributes.

Fiber attribute models

The candidate models for estimating wood fiber attributes were ranked according to their AICc scores (Table 4). The "STEM" models provided essentially no support for the top-ranking models with deltas (Δ_i; AICc differences) greater than 10. Adding crown measurements into the "STEM" models slightly reduced the AICc scores, but the contribution of the "STEM+CROWN" models was limited with deltas greater than 10, except for estimating coarseness (Δ_i=6; w_{BEST}/w_i=25 times less support than the top-ranking model). The base of live crown accounted for 33%, 54%, 65%, and 51% of the explained variation in basic wood density, coarseness, MFA, and MOE, respectively. The "CORE" models were always more parsimonious than the "STEM+CROWN" models for estimating wood fiber attributes. The "CORE" models provided substantial support for estimating coarseness (Δ_i=2; w_{BEST}/w_i=3), less support for estimating fiber length (Δ_i=8; w_{BEST}/w_i=52), MFA (Δ_i=6; w_{BEST}/w_i=19), and MOE (Δ_i=3; w_{BEST}/w_i=4), and essentially no support for estimating wood density (Δ_i=16; w_{BEST}/w_i=3 294). The "STEM+CROWN+CORE" model was the top-ranking model for estimating wood density, but its contribution was limited for estimating other wood fiber attributes. The "CORE" and "STEM+CROWN+CORE" models were the same for coarseness, MFA, and MOE, with only core measurements retained in the best models.

Predictive models were successfully developed to estimate wood fiber attributes using only TLS metrics (Table 4). The "TLS" models provided substantial support for estimating MFA (Δ_i=1; w_{BEST}/w_i=2) and MOE (Δ_i=2; w_{BEST}/w_i=2), less support for estimating coarseness (Δ_i=7; w_{BEST}/w_i=30) and fiber length (Δ_i=4; w_{BEST}/w_i=8), and essentially no support for estimating wood density (Δ_i=21; w_{BEST}/w_i=36 316). The crown volume (TLS_CR_VOL) accounted for 48% of the explained variation in basic wood density. The structural characteristics of the canopy height model (CHM_RUMPLE, CHM_STD) accounted for 56%, 67%, 25%, and 30% of the explained variation in coarseness, fiber length, MFA, and MOE, respectively. The mean distance between trees (TLS_DISTANCE) accounted for 55% and 48% of the explained variation in MFA and MOE, respectively. Adding TLS metrics to the "STEM+CROWN" models reduced the AICc scores for estimating wood density and coarseness. The "STEM+CROWN+TLS" models provided substantial support for estimating coarseness (Δ_i=1; w_{BEST}/w_i=1) but no support for estimating basic wood density (Δ_i=13; w_{BEST}/w_i=773). The "TLS" and "STEM+CROWN+TLS" models were the same for fiber length, MFA, and MOE, with only TLS metrics retained in the best models. Adding TLS metrics into the "STEM+CROWN+CORE" models was more conclusive. The "STEM+CROWN+CORE+TLS" models were indeed the top-ranking models for estimating coarseness, fiber length, MFA, and MOE. The TLS metrics accounting for 37%, 68%, 42%, and 61% of the explained variation in coarseness, fiber length, MFA, and MOE, respectively. The "STEM+CROWN+CORE" and "STEM+CROWN+CORE+TLS" models were the same for wood density as no TLS metrics were retained in the best models.

Discussion

The contribution of TLS to the estimation of wood fiber attributes at the tree level was demonstrated in black spruce. The “TLS” models, developed using only TLS metrics, accounted for 47%, 33%, 51%, 44%, and 52% of variance in wood density, coarseness, fiber length, MFA, and MOE, respectively, with root mean square error (RMSE) and normalized RMSE values of 46 kg/m^3 (17%), 37 µg/m (17%), 0.20 mm (16%), 3.5^o (15%), 2.3 GPa (15%). These “TLS” models were the second top-ranking models for estimating fiber length, MFA, and MOE. In addition, at least one TLS metric was retained in the top-ranking models for estimating coarseness, fiber length, MFA, and MOE. The contribution of TLS was less obvious for estimating wood density when the models included core measurements. However, in the field, it is only possible to measure the crown and collect increment cores on a few trees within a plot. An inventory using only TLS data would therefore be preferred over conventional inventories to predict the fiber attributes at the tree level if TLS data could be available for all trees within a plot. The “TLS” models were indeed always more parsimonious than “STEM” models for estimating the attributes of wood fiber. The TLS models were also more parsimonious than the “STEM+CROWN+CORE” models for estimating fiber length, MFA, and MOE.

As the top-ranking models included core measurements, it was not surprising that TLS metrics added little additional information, particularly for wood density. The core measurements take into account the past growth of the tree and the level of maturity of the cambium. The first growth rings from the pith form the juvenile wood, which has inferior physical and mechanical properties than those found in the mature wood of the same tree (Panshin and de Zeeuw 1980). The maturity of the cambium at a given height is thus related to the number of rings, which turned out to be one of the most important covariates in our study. These results were consistent with previously published results for black spruce wood properties (Alteyrac et al. 2006; Giroud et al. 2016; Pokharel et al. 2014). A negative influence of the radial growth on the wood fiber attributes at breast height was also observed in the current study. This inverse relationship is known in black spruce, particularly for wood density (Giroud et al. 2016; Groot and Luther 2015). Ring width is indeed negatively related to the proportion of latewood in softwoods (Panshin and de Zeeuw 1980). A large part of the variation in trees may also be due to cambium responses to different growth stresses over the life of a tree, such as drought or wind stress, which directly influence the MFA and other wood properties (Donaldson 2008).

Contrary to our expectations, detailed crown metrics derived from TLS point clouds were not more related with wood fiber attributes than field crown metrics. The influence of canopy competition indices was also limited. However, some biological interpretation can be done. Based on the 3D reconstruction of the crown, we confirmed, for example, that trees with large crowns produced less dense wood as suggested by Larson (1969). Wood fiber attributes were also positively influenced by the base of live crown. As the tree crown rises with time, the cambium at a given height becomes less subject to direct influence of the crown, and mature wood is formed (Panshin and de Zeeuw 1980). However, manual extraction of this metric from the TLS point cloud has limitations. The base of live crowns measured in the field seemed more accurate, as shown by the higher correlations obtained with wood fiber attributes. An automatic procedure to extract this metric could improve the accuracy and possibly the overall contribution of TLS. The sampling method may partly explain the limited influence of crown metrics. Indeed, wood fiber attributes were measured from pith to bark at breast height, but these attributes also vary longitudinally within a tree (Panshin and de Zeeuw 1980). Whole-tree estimates could be used to better characterize the relationships with crown metrics, or other tree-level metrics, and potentially improve the predictive ability of the models. Breast-height estimates are nevertheless considered moderate to good predictors for the whole tree (Evans et al. 2000).

Competition metrics derived from TLS were also interesting covariates for assessing wood fiber attributes. As expected, trees suppressed by their immediate neighbors had better physical and mechanical properties (Johansson 1993; Yang and Hazenberg 1994). Better wood properties were also found in trees growing in an immediate environment characterized by an irregular forest structure. Standard deviation and rumple index of the local canopy height models were indeed positively and strongly correlated with the age of target trees ($r \sim 0.7$; results not shown). Although there has been limited study of the influence of terrain on wood attributes because of the difficulty in accurately measuring terrain features, we found that trees growing on sloping ground produced wood with lower physical and mechanical properties. These results were unexpected because compression wood is usually observed in such growth conditions. However, the variability of the mean slope was relatively limited in the current study.

Conclusion

The contribution of TLS for estimating wood fiber attributes at the tree level was investigated for black spruce trees growing in Newfoundland, Canada. This study demonstrated that more accurate characterization of the tree, its crown, and its immediate environment using TLS metrics improved the predictive ability of the models for estimating most wood fiber attributes of black spruce. An inventory using only TLS data would be preferred over conventional inventories to predict fiber attributes at the tree level, particularly if TLS data were available for all trees in a plot. Terrestrial laser scanning provides information beyond what is typically available from conventional inventories, however, there remain some issues to address for operational use, such as reducing the effects of occlusion and automating processes to extract metrics at the tree level. Nonetheless, TLS data acquisition and processing is becoming more and more efficient, suggesting great potential for application in forestry in the coming years. Finally, this study was developed as a proof-of-concept to evaluate the contribution of TLS for estimating wood fiber attributes at the tree level. More sampled trees and sites would be required to develop models that could be generalized to any black spruce site.

Acknowledgements

Field data collection and TLS data acquisition and preprocessing were carried out with funding and research support provided by the Newfoundland Fibre Project and by the Canadian Wood Fibre Centre. The fiber attribute database was provided by FPInnovations under the Forest Industry Competitive Advantage Project led by Corner Brook Pulp and Paper Limited. The extraction of TLS metrics was funded by the Fonds de recherche du Québec – Nature et technologies. The authors would like to thank all project members and are especially grateful to Danny Blanchette, Université de Sherbrooke, for the extraction of TLS metrics, Olivier van Lier, Canadian Forest Service, for field logistics and organization of the field and fiber attribute data, and Marie-Claude Lambert, Ministère des Forêts, de la Faune et des Parcs du Québec, for statistical support. We also thank Caroline Simpson, Canadian Forest Service, for editing this manuscript and anonymous reviewers for their helpful comments and suggestions.

References

Alemdag, I.S. 1984. Wood density variation of 28 tree species from Ontario. Natural Resources Canada, Canadian Forest Service, Petawawa, ON. Information Report PI-X-45F.

Alteyrac, J., Cloutier, A., and Zhang, S.Y. 2006. Characterization of juvenile wood to mature wood transition age in black spruce (*Picea mariana* (Mill.) B.S.P.) at different stand densities and sampling heights. Wood Sci. Technol. **40**(2): 124–138.

Blanchette, D., Fournier, R.A., Luther, J.E., and Côté, J.F. 2015. Predicting wood fiber attributes using local-scale metrics from terrestrial LiDAR data: a case study of Newfoundland conifer species. For. Ecol. Manage. **347**: 116–129.

Burnham, K.P., and Anderson, D.R. 2003. Model selection and multimodel inference: a practical information-theoretic approach. Springer Science & Business Media, New York.

Clark, P.J., and Evans, F.C. 1954. Distance to nearest neighbor as a measure of spatial relationships in populations. Ecology **35**(4): 445–453.

Defo, M., Duchesne, I., and Stewart, J. 2015. A review of the current state of wood quality modelling and decision support systems in Canada. Natural Resources Canada, Canadian Forest Service – Canadian Wood Fibre Centre. Laurentian Forestry Centre, Québec, QC. Information Report FI-X-012.

Donaldson, L. 2008. Microfibril angle: measurement, variation and relationships – a review. IAWA J. **29**(4): 345–386.

Evans, R. 1994. Rapid measurement of the transverse dimensions of tracheids in radial wood sections from *Pinus radiata*. Holzforschung **48**(2): 168–172.

Evans, R. 2006. Wood stiffness by X-ray diffractometry. Chapter 11. *In* : Characterization of the cellulosic cell wall. *Edited by* Stokke D.D. and L. H. Groom. Proceedings of a workshop cosponsored by the USDA Forest Service - Southern Research Station, the Society of Wood Science and Technology, and Iowa State University, Grand Lake, Colorado, USA, August 25–27 2003. Blackwell Publishing, Hoboken, NJ. pp. 138–146.

Evans, R., Stringer S. and Kibblewhite R.P. 2000. Variation of microfibril angle, density and fibre orientation in twenty-nine *Eucalyptus nitens* trees. Appita J. **53**(5): 450–457.

Giroud, G., Bégin, J., Defo, M., and Ung, C.H. 2016. Ecogeographic variation in black spruce wood properties across Quebec's boreal forest. For. Ecol. Manage. **378**: 131–143.

Giroud, G., Bégin, J., Defo, M., and Ung, C.H. 2017. Regional variation in wood density and modulus of elasticity of Quebec's main boreal tree species. For. Ecol. Manage. **400**: 289–299.

Government of Newfoundland and Labrador. 2015. Newfoundland and Labrador Wood Products Industry. 2014 Summary. 2015 Issue. Forestry & Agrifoods Agency, Corner Brook, NL. Available from http://www.faa.gov.nl.ca/publications/pdf/Wood_Prod_Ind_2014.pdf [accessed 2018-08-07].

Government of Newfoundland and Labrador. 2018a. Forest Products Industry [online]. Available from http://www.faa.gov.nl.ca/forestry/support/services.html [accessed 2018-08-07].

Government of Newfoundland and Labrador. 2018b. Forest Types [online]. Available from http://www.faa.gov.nl.ca/forestry/our_forest/forest_types.html [accessed 2018-08-07].

Groot, A., and Luther, J.E. 2015. Hierarchical analysis of black spruce and balsam fir wood density in Newfoundland. Can. J. For. Res. **45**(7): 805–816.

Groot, A., Cortini, F., and Wulder, M.A. 2015. Crown-fibre attribute relationships for enhanced forest inventory: Progress and prospects. For. Chron. **91**(3): 266–279.

Huang, H., Gong, P., Cheng, X., Clinton, N., Cao, C., Ni, W., Li, Z., and Wang, L. 2009. Forest structural parameter extraction using terrestrial LiDAR. *In* Proceedings of SilviLaser 2009: 9^{th} international conference on LiDAR applications for assessing forest ecosystems, Texas A&M University, Austin, TX, October 14–16, 2009.

Johansson, K. 1993. Influence of initial spacing and tree class on the basic density of *Picea abies*. Scand. J. Forest Res. **8**(1–4): 18–27.

Kane, V.R., McGaughey, R.J., Bakker, J.D., Gersonde, R.F., Lutz, J.A., and Franklin, J.F. 2010. Comparisons between field-and LiDAR-based measures of stand structural complexity. Can. J. For. Res. **40**(4): 761–773.

Lafarge, T., and Pateiro-Lopez, B. 2017. R package “Alphashape3d”. Implementation of the 3D alpha-shape for the reconstruction of 3D sets from a point cloud. Available from https://cran.r-project.org/web/packages/alphashape3d/alphashape3d.pdf [accessed 2018-08-07].

Larson P.R. 1969. Wood formation and the concept of wood quality. Yale University School of Forestry, New Haven, CT. Bull. No.74.

Lecigne, B., Delagrange, S., and Messier, C. 2015. R package “VoxR”. Metrics extraction of trees from T-LiDAR data. Available from https://cran.r-project.org/web/packages/VoxR/VoxR.pdf [accessed 2018-08-07].

Lessard, E., Fournier, R.A., Luther, J.E., Mazerolle, M.J., and van Lier, O.R. 2014. Modeling wood fiber attributes using forest inventory and environmental data for Newfoundland’s boreal forest. For. Ecol. Manage. **313**: 307–318.

Li, B., Li, H., Zha, Q., Bandekar, R., Alsaggaf, A., and Ni, Y. 2011. Review: effects of wood quality and refining process on TMP pulp and paper quality. BioResources **6**(3): 3569–3584.

Luther, J.E., Skinner, R., Fournier, R.A., van Lier, O.R., Bowers, W.W., Coté, J.-F., Hopkinson, C., and Moulton, T. 2014. Predicting wood quantity and quality attributes of balsam fir and black spruce using airborne laser scanner data. Forestry **87**: 313–326.

Martin-Ducup, O., Robert, S., and Fournier, R.A. 2016. Response of sugar maple (*Acer saccharum*, Marsh.) tree crown structure to competition in pure versus mixed stands. For. Ecol. Manage. **374**: 20–32.

Nakagawa, S., and Schielzeth, H. 2013. A general and simple method for obtaining R^2 from generalized linear mixed-effects models. Methods Ecol. Evol. **4**(2): 133–142.

Natural Resources Canada. 2010. The principal attributes of Canadian wood fibre. Natural Resources Canada, Canadian Forest Service – Canadian Wood Fibre Centre. Ottawa, ON.

Othmani, A., Piboule, A., Krebs, M., Stolz, C., and Voon, L.L.Y. 2011. Towards automated and operational forest inventories with T-Lidar. *In* Proceedings of SilviLaser 2011: 11th international Conference on LiDAR applications for assessing forest ecosystems, University of Tasmania, Hobart, Australia. October 16–20, 2011. Available from http://www.iufro.org/download/file/8239/5065/40205-silvilaser2011_pdf [accessed 2018-08-07]. pp. 465–473.

Panshin, A.J., and de Zeeuw, C. 1980. Textbook of wood technology. Structure, identification, properties, and uses of the commercial woods of the United States and Canada. 4th edition. McGraw-Hill Book Company, New York. 722 p.

Pokharel, B., Dech, J.P., Groot, A., and Pitt, D. 2014. Ecosite-based predictive modeling of black spruce (*Picea mariana*) wood quality attributes in boreal Ontario. Can. J. For. Res. **44**(5): 465–475.

Pokharel, B., Groot, A., Pitt, D.G., Woods, M., and Dech, J.P. 2016. Predictive modeling of black spruce (*Picea mariana* (Mill.) BSP) wood density using stand structure variables derived from airborne LiDAR data in boreal forests of Ontario. Forests **7**(12): 311.

R Core Team. 2018. R: A Language and Environment for Statistical Computing. R Foundation for Statistical Computing, Vienna, Austria. Available from http://www.R-project.org [accessed 2018-08-07].

Robertson, G., Olson, J., Allen, P., Chan, B., and Seth, R. 1999. Measurement of fiber length, coarseness, and shape with the fiber quality analyzer. Tappi J. **82**: 93–98.

Siau, J.F. 1995. Wood: influence of moisture on physical properties. Dept. of Wood Science and Forest Products, Virginia Polytechnic Institute and State University, Blacksburg, VA.

Yang, K.C., and Hazenberg, G. 1994. Impact of spacing on tracheid length, relative density, and growth-rate of juvenile wood and mature wood in *Picea mariana*. Can. J. For. Res. **24**(5): 996–1007.

Table captions

Table 1. Site characteristics and descriptive statistics of wood fiber attributes.

Table 2. Descriptive statistics of wood fiber attributes, field, and TLS metrics (n = 69 visible target trees). The different groups of covariates are shown ("CORE", "STEM", "CROWN", and "TLS").

Table 3. Pearson's correlation for wood fiber attributes, field, and TLS metrics. Highly significant correlations ($P < 0.001$) are shown in bold.

Table 4. Top-ranking models of wood fiber attributes. Differences in AICc (Δi), AICc weight (wi), pseudo-R2, and RMSE are provided. Signs of parameter coefficients (S1, S2, S3) and percentages of variance explained by the model (P1, P2, P3) are shown for each covariate (V1, V2, V3). TLS metrics are shown in bold.

Table 1. Site characteristics and descriptive statistics of wood fiber attributes

Site ID	TLS visible target tree count	Latitude N	Longitude W	Elevation (m)	Slope (%)	Black spruce (%)	Tree age		BD (kg/m³)		COA (μg/m)		FL (mm)		MFA (°)		MOE (GPa)	
							mean	c.v.	mean	c.v.	mean	c.v.	mean	c.v.	mean	c.v.	mean	c.v.
18900805	4	49°01"10	54°09"40	98	0	98	70	10%	590.9	7%	401.9	11%	2.4	7%	12.6	22%	17.2	16%
18901205	6	48°59"40	53°58"17	76	6	100	32	8%	538.4	10%	358.3	6%	2.0	7%	16.0	25%	13.8	14%
18905502	3	48°18"09	53°44"22	110	5	69	23	9%	450.2	3%	305.4	11%	1.9	6%	18.5	13%	9.9	17%
19200416	3	49°34"36	57°03"20	130	6	69	48	9%	493.3	5%	318.0	5%	2.0	7%	21.1	27%	10.2	21%
19203116	3	49°43"58	57°16"05	340	15	77	28	5%	443.4	4%	313.2	10%	1.8	6%	27.3	19%	7.0	23%
19400404	3	48°33"12	54°56"28	232	0	91	97	30%	561.6	1%	384.5	7%	2.2	3%	16.0	10%	13.9	5%
19400504	7	48°31"13	54°57"37	220	0	86	120	22%	621.2	6%	383.0	9%	2.1	10%	12.8	28%	17.2	10%
19400706	6	48°51"25	54°35"45	189	3	98	71	20%	554.5	4%	395.7	5%	2.2	8%	12.8	17%	15.4	7%
19401411	5	48°48"37	56°00"44	198	5	94	86	6%	512.3	9%	375.9	9%	2.4	7%	11.4	18%	15.4	17%
19401611	4	48°35"38	55°57"07	192	12	82	102	11%	546.9	6%	404.0	7%	2.7	3%	14.0	25%	14.9	14%
19401911	4	48°35"25	55°34"14	175	3	97	148	11%	599.6	12%	423.4	11%	2.7	7%	10.4	19%	18.2	7%
19500110	3	49°04"55	55°57"10	138	0	99	67	7%	572.5	17%	411.9	17%	2.4	7%	12.0	8%	16.5	21%
19500508	6	49°11"25	54°39"20	61	0	100	75	10%	530.6	7%	361.2	9%	2.3	9%	17.6	15%	12.7	18%
19501112	9	48°44"52	56°45"54	158	5	95	78	14%	594.4	8%	410.9	8%	2.4	7%	15.8	23%	14.9	16%
19501309	1	49°53"14	56°13"02	80	5	78	54	-	465.8	-	344.2	-	2.1	-	18.4	-	10.7	-
19502309	2	49°24"25	55°38"24	131	30	37	73	4%	595.4	2%	433.8	8%	2.7	5%	11.8	19%	17.3	12%

Table 2. Descriptive statistics of wood fiber attributes, field, and TLS metrics (n = 69 visible target trees). The different groups of covariates are shown ("CORE", "STEM", "CROWN", and "TLS")

Variable		Description	Abbreviation	mean	s.d.	min.	max.	CORE	STEM	CROWN	TLS
Core-level	response	Basic wood density (kg/m^3)	BD	553.2	62.9	421.2	699.1				
	response	Coarseness (µg/m)	COA	380.8	45.6	267.9	491.4				
	response	Fiber length (mm)	FL	2.3	0.3	1.7	2.9				
	response	Microfibril angle (°)	MFA	15.1	4.7	8.8	32.2				
	response	Modulus of elasticity (GPa)	MOE	14.5	3.3	5.8	20.8				
	field data	Ring number	RN	77.0	34.1	21.0	165.0	X			
	field data	Log transformation of ring number	RNLN	4.2	0.5	3.0	5.1	X			
	field data	Ring width (mm)	RW	0.9	0.6	0.3	3.0	X			
Tree-level	field data	Diameter at breast height (cm)	DBH	14.2	3.7	8.6	24.5		X		
	field data	Tree height (m)	TH	11.1	2.4	6.8	16.3		X		
	field data	Slenderness, ratio of tree height to DBH (m/cm)	HD	0.8	0.1	0.5	1.1		X		
	field data	Basal area of larger trees (m^2/ha)	BAL	18.4	11.3	0.5	52.9		X		
	field data	Base of live crown (m)	CR_BLC	6.4	2.4	1.0	10.5			X	
	field data	Crown length (m)	CR_LGT	4.6	2.1	0.4	9.7			X	
	TLS data	Diameter at breast height (cm)	TLS_DBH	15.4	3.6	9.4	25.2				X
	TLS data	Tree height (m)	TLS_TH	11.5	2.4	6.9	17.0				X
	TLS data	Slenderness, ratio of tree height to DBH (m/cm)	TLS_HD	0.8	0.1	0.4	1.1				X
	TLS data	Base of live crown (m)	TLS_CR_BLC	4.6	2.4	0.6	9.7				X
	TLS data	Crown length (m)	TLS_CR_LGT	6.9	2.7	2.8	13.4				X
	TLS data	Crown surface area (m^2)	TLS_CR_SA	44.6	29.8	11.4	150.3				X
	TLS data	Crown density (%)	TLS_CR_DEN	20.7	6.3	9.7	39.5				X
	TLS data	Crown volume (m^3)	TLS_CR_VOL	11.9	10.1	1.8	52.2				X
	TLS data	Canopy pressure index	CPI	3.7	1.6	0.8	9.8				X
	TLS data	Canopy heterogeneity index	CHI	1.5	0.2	0.7	1.8				X
	TLS data	Canopy density index	CDI	0.23	0.14	0.00	0.55				X
	TLS data	Canopy height model - mean (m)	CHM_MEAN	8.2	1.9	4.3	11.9				X
	TLS data	Canopy height model - standard deviation (m)	CHM_STD	2.1	0.8	0.9	3.5				X
	TLS data	Canopy height model - volume to area ratio (m^3/m^2)	CHM_RATIO	367.1	199.3	85.1	823.9				X
	TLS data	Canopy height model - rumple index (unitless)	CHM_RUMPLE	4.6	1.2	2.7	7.4				X
	TLS data	Digital elevation model - standard deviation (m)	DEM_EL_STD	0.2	0.1	0.0	0.4				X
	TLS data	Digital elevation model - relative difference (unitless)	DEM_EL_DIF	0.7	0.4	0.2	1.8				X
	TLS data	Digital elevation model - rumple index (unitless)	DEM_EL_RUMPLE	1.01	0.01	1.00	1.03				X
	TLS data	Digital elevation model - mean slope (°)	DEM_SL_MEAN	5.0	2.9	1.4	12.7				X
	TLS data	Digital elevation model - standard deviation of the slope (°)	DEM_SL_STD	1.7	0.8	0.8	4.9				X
	TLS data	Nearest neighbor ratio (m/m, therefore unitless)	TLS_RATIO	1.2	0.3	0.6	2.0				X
	TLS data	Mean distance between trees (m)	TLS_DISTANCE	1.0	0.4	0.5	2.5				X

Table 3. Pearson's correlation for wood fiber attributes, field, and TLS metrics. Highly significant correlations ($P < 0.001$) are shown in bold

Variable		Description	BD	COA	FL	MFA	MOE
Core-level	response	Basic wood density (kg/m^3)	**1.00**				
	response	Coarseness (µg/m)	**0.65**	**1.00**			
	response	Fiber length (mm)	0.29	**0.61**	**1.00**		
	response	Microfibril angle (°)	**-0.38**	**-0.50**	**-0.58**	**1.00**	
	response	Modulus of elasticity (GPa)	**0.73**	**0.67**	**0.55**	**-0.89**	**1.00**
	field data	Ring number	**0.47**	**0.47**	**0.56**	**-0.54**	**0.59**
	field data	Log transformation of ring number	**0.53**	**0.53**	**0.63**	**-0.55**	**0.62**
	field data	Ring width (mm)	**-0.70**	**-0.58**	**-0.56**	**0.56**	**-0.70**
Tree-level	field data	Diameter at breast height (cm)	**-0.39**	n.s.	0.26	n.s.	n.s.
	field data	Tree height (m)	n.s.	n.s.	**0.50**	**-0.32**	n.s.
	field data	Slenderness, ratio of tree height to DBH (m/cm)	**0.58**	**0.34**	n.s.	-0.27	**0.44**
	field data	Basal area of larger trees (m^2/ha)	**0.32**	n.s.	n.s.	n.s.	n.s.
	field data	Base of live crown (m)	**0.36**	**0.46**	**0.46**	**-0.41**	**0.43**
	field data	Crown length (m)	**-0.34**	n.s.	n.s.	n.s.	n.s.
	TLS data	Base of live crown (m)	n.s.	0.29	n.s.	-0.28	0.24
	TLS data	Crown length (m)	n.s.	n.s.	**0.33**	n.s.	n.s.
	TLS data	Crown density (%)	n.s.	n.s.	**-0.34**	n.s.	n.s.
	TLS data	Crown volume (m^3)	**-0.42**	n.s.	n.s.	n.s.	-0.28
	TLS data	Canopy pressure index	**0.39**	n.s.	n.s.	n.s.	0.31
	TLS data	Canopy heterogeneity index	**0.41**	**0.32**	n.s.	**-0.42**	**0.43**
	TLS data	Canopy density index	**0.35**	n.s.	n.s.	n.s.	0.29
	TLS data	Canopy height model - standard deviation (m)	n.s.	0.26	**0.50**	**-0.32**	**0.34**
	TLS data	Canopy height model - rumple index (unitless)	0.26	0.29	**0.50**	**-0.33**	**0.37**
	TLS data	Digital elevation model - rumple index (unitless)	**-0.44**	**-0.31**	n.s.	**0.38**	**-0.43**
	TLS data	Digital elevation model - mean slope (°)	**-0.47**	**-0.33**	-0.24	**0.35**	**-0.43**
	TLS data	Nearest neighbor ratio (m/m, therefore unitless)	**-0.37**	**-0.49**	**-0.65**	**0.51**	**-0.54**
	TLS data	Mean distance between trees (m)	**-0.41**	**-0.47**	**-0.38**	**0.49**	**-0.52**

Table 4. Top-ranking models of wood fiber attributes. Differences in AICc (Δ_i), AICc weight (w_i), pseudo-R^2, and RMSE are provided. Signs of parameter coefficients (S1, S2, S3) and percentages of variance explained by the model (P1, P2, P3) are shown for each covariate (V1, V2, V3). TLS metrics are shown in bold

Wood fiber attribute	**Model set**	**AIC_C**	**Δ_i**	**w_i**	**R^2**	**RMSE**	**V1**	**S1**	**P1**	**V2**	**S2**	**P2**	**V3**	**S3**	**P3**
Basic wood density (kg/m3)	STEM+CROWN+CORE	712	0	0.500	0.61	39.5	RNLN	+	46%	HD	+	35%	TH	-	19%
	STEM+CROWN+CORE+TLS	712	0	0.500	0.61	39.5	RNLN	+	46%	HD	+	35%	TH	-	19%
	STEM+CROWN+TLS	725	13	0.001	0.54	42.8	DBHLN	-	47%	**CHM_RUMPLE**	+	35%	**DEM_SL_MEAN**	-	18%
	CORE	728	16	0.000	0.48	45.3	RW	-	100%						
	STEM+CROWN	731	18	0.000	0.36	50.3	DBH	-	44%	CR_BLC	+	33%	CR_LGT	+	22%
	TLS	733	21	0.000	0.47	46.0	**TLS_CR_VOL**	-	48%	**DEM_SL_MEAN**	-	28%	**TLS_CR_LGT**	+	24%
	STEM	734	22	0.000	0.33	51.5	HD	+	100%						
Coarseness (µg/m)	STEM+CROWN+CORE+TLS	698	0	0.403	0.37	36.2	RNLN	+	63%	**TLS_DISTANCE**	-	37%			
	STEM+CROWN+TLS	698	1	0.284	0.38	35.8	**TLS_CR_DEN**	-	40%	**TLS_DISTANCE**	-	35%	CR_BLC	+	25%
	STEM+CROWN+CORE	700	2	0.141	0.33	37.4	RW	-	100%						
	CORE	700	2	0.141	0.33	37.4	RW	-	100%						
	STEM+CROWN	704	6	0.016	0.13	42.4	CR_BLC	+	54%	CR_LGT	+	46%			
	TLS	705	7	0.013	0.33	37.4	**CHM_RUMPLE**	+	56%	**TLS_CR_DEN**	+	29%	**CPI**	+	14%
	STEM	710	12	0.001	0.04	44.6	TH	+	100%						
Fiber length (mm)	STEM+CROWN+CORE+TLS	-25	0	0.760	0.47	0.21	**TLS_CR_VOL**	+	45%	RW	-	32%	**CHM_MEAN**	+	23%
	TLS	-21	4	0.093	0.51	0.20	**CHM_STD**	+	67%	**TLS_CR_DEN**	+	21%	**TLS_DISTANCE**	+	12%
	STEM+CROWN+TLS	-21	4	0.093	0.51	0.20	**CHM_STD**	+	67%	**TLS_CR_DEN**	+	21%	**TLS_DISTANCE**	+	12%
	STEM+CROWN+CORE	-19	6	0.036	0.42	0.22	RW	-	61%	DBH	+	39%			
	CORE	-17	8	0.015	0.39	0.22	RNLN	+	100%						
	STEM+CROWN	-13	12	0.002	0.24	0.25	TH	+	100%						
	STEM	-13	12	0.002	0.24	0.25	TH	+	100%						
Microfibril angle (°)	STEM+CROWN+CORE+TLS	375	0	0.431	0.42	3.6	RN	-	58%	**TLS_DISTANCE**	+	42%			
	TLS	376	1	0.262	0.44	3.5	**TLS_DISTANCE**	+	55%	**CHM_STD**	-	25%	**DEM_EL_RUMPLE**	+	21%
	STEM+CROWN+TLS	376	1	0.262	0.44	3.5	**TLS_DISTANCE**	+	55%	**CHM_STD**	-	25%	**DEM_EL_RUMPLE**	+	21%
	STEM+CROWN+CORE	381	6	0.023	0.30	3.9	RNLN	-	100%						
	CORE	381	6	0.023	0.30	3.9	RNLN	-	100%						
	STEM+CROWN	390	15	0.000	0.15	4.3	CR_BLC	-	65%	CR_LGT	-	35%			
	STEM	391	16	0.000	0.09	4.5	TH	-	100%						
Modulus of elasticity (GPa)	STEM+CROWN+CORE+TLS	316	0	0.424	0.52	2.3	RW	-	39%	**DEM_EL_RUMPLE**	-	31%	**TLS_RATIO**	-	29%
	TLS	318	2	0.172	0.52	2.3	**TLS_DISTANCE**	-	48%	**CHM_RUMPLE**	+	30%	**DEM_EL_RUMPLE**	-	22%
	STEM+CROWN+TLS	318	2	0.172	0.52	2.3	**TLS_DISTANCE**	-	48%	**CHM_RUMPLE**	+	30%	**DEM_EL_RUMPLE**	-	22%
	STEM+CROWN+CORE	319	3	0.116	0.48	2.3	RW	-	100%						
	CORE	319	3	0.116	0.48	2.3	RW	-	100%						
	STEM+CROWN	330	14	0.000	0.22	2.9	CR_BLC	+	51%	CR_LGT	+	31%	DBH	-	18%
	STEM	333	17	0.000	0.20	2.9	TH	+	59%	DBH	-	41%			

Figure captions

Figure 1. Sampling configuration for the TLS data acquisition (Blanchette et al. 2015). The term "sampled fiber tree" refers to a target tree. The term "area of interest" refers to a TLS scene including all the target trees.

Figure 2. TLS data processing: (A) extraction of the scene using an upside-down cone placed at the tree base with a 30º opening angle. The cylinder diameter was estimated as a function of the highest point of the canopy; (B and C) extraction of the target tree using a semi-automatic procedure in Computree software; (D) reconstruction of the crown using the ‘‘alphashape3d" R package; (E) extraction of the immediate vegetation, surrounding each target tree, using an upside-down cone placed at the crown base with a 30° opening angle.

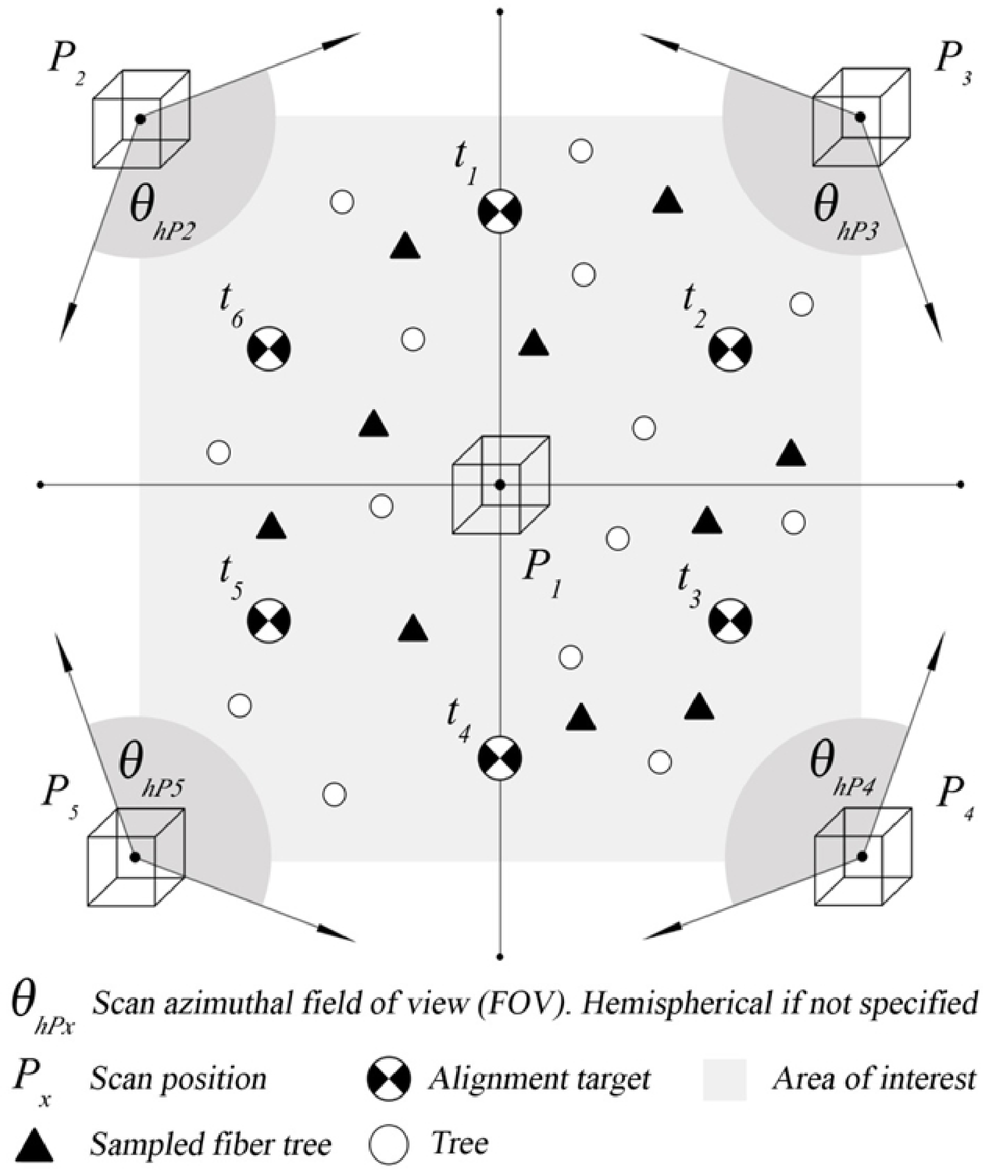

Figure 1. Sampling configuration for the TLS data acquisition (Blanchette et al. 2015). The term "sampled fiber tree" refers to a target tree. The term "area of interest" refers to a TLS scene including all the target trees.

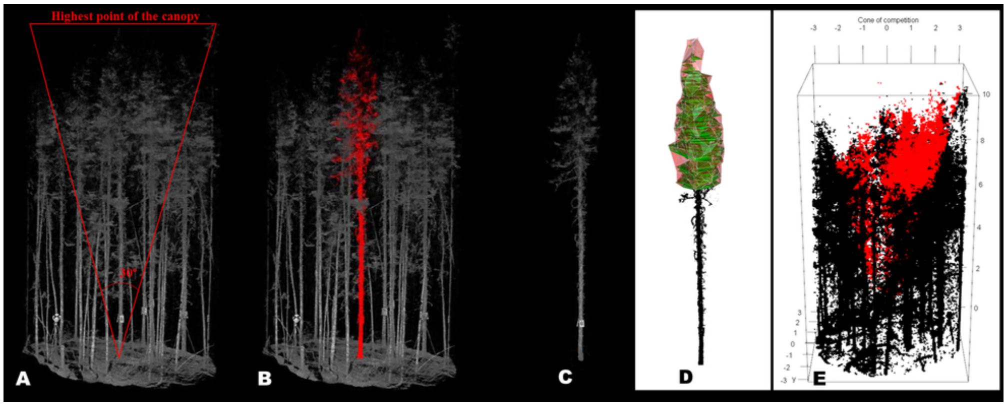

Figure 2. TLS data processing: (A) extraction of the scene using an upside-down cone placed at the tree base with a 30º opening angle. The cylinder diameter was estimated as a function of the highest point of the canopy; (B and C) extraction of the target tree using a semi-automatic procedure in Computree software; (D) reconstruction of the crown using the "alphashape3d" R package; (E) extraction of the immediate vegetation, surrounding each target tree, using an upside-down cone placed at the crown base with a 30º opening angle.

83x33mm (300 x 300 DPI)